

Damaging effect of ischemia on the development of retinal organoids derived from human embryonic stem cells

Yu-Han Yan^{1,2}, Hong-Yu Li³, Li-Xiong Gao², Wen Li^{1,2}, Ling-Ping Zhao³, Quan Zeng³, Yu Luo^{1,2}, Tian-Tian Cui³, Ru-Ge Zang³, Zi Ye^{1,2}, Jia-Fei Xi³, Wen Yue³, Zhao-Hui Li^{1,2}

¹Medical School of Chinese PLA, Beijing 100853, China

²Senior Department of Ophthalmology, the Third Medical Center of Chinese PLA General Hospital, Beijing 100039, China

³Beijing Institute of Radiation Medicine, Beijing 100850, China

Co-first Authors: Yu-Han Yan and Hong-Yu Li

Correspondence to: Zhao-Hui Li. Senior Department of Ophthalmology, Chinese PLA General Hospital, Beijing 100853, China. zhaohuili202104@163.com; Wen Yue. Beijing Institute of Radiation Medicine, Beijing 100850, China. yuewen@bmi.ac.cn

Received: 2024-10-10 Accepted: 2025-04-25

Abstract

• **AIM:** To explore the changes in early retinal development after the occurrence of ischemia.

• **METHODS:** Human retinal organoids (hROs) of day 18 or day 30 were treated with oxygen-glucose deprivation and reperfusion (OGD/R) to simulate the retinal ischemia. All hROs were maintained normally until day 60 to evaluate changes in ischemic injuries during retinal development. Paraffin section staining was used for detecting changes in organoid structure and cell number. Real-time quantitative polymerase chain reaction (RT-qPCR) and Western blot (WB) analyses were used to observe the change in the expression of retinal cell markers.

• **RESULTS:** In hROs, OGD/R induced the decrease of proliferating cells, inhibited the expression of proliferated marker Ki67 and promoted early apoptosis of retinal cells ($P < 0.05$). Under OGD/R condition, the progenitor cell layer and ganglion cell layer of hROs lost normal structure, and the number of neural stem cells (SOX2⁺), retinal progenitor cells (CHX10⁺) and retinal ganglion cells (TUJ1⁺/BRN3⁺/ATOH7⁺) decreased ($P < 0.05$). The expression of corresponding retinal cell markers also decreased ($P < 0.05$). Organoids treated with OGD/R on day 30 had similar injuries in retinal structure and retinal cell markers

to those on day 18. Long-term observations revealed that day 18-treated organoids remained disorganized progenitor and ganglion cell layers by day 60, with no recovery in proliferating cell nuclear antigen (PCNA) protein expression. RT-qPCR showed persistently low Ki67 transcription levels ($P < 0.001$), while other retinal cell markers recovered or exceeded normal levels, indicating a limited self-repair happened in the development of hROs. In contrast, day 30-treated organoids exhibited normal structure and marker expression by day 60, with transcription levels of retinal cell markers returning to normal ($P > 0.05$), demonstrating complete recovery from OGD/R damage.

• **CONCLUSION:** Retinal ischemia damage the retinal development in the short-term. After the restoration of retinal blood supply, the retinal ischemic damage can be recovered during subsequent development. However, retinal ischemic injuries at different developmental stages exhibit varying degrees of reversibility. The earlier ischemic injury occurs, the more difficult it is to repair retinal cell and structure damage.

• **KEYWORDS:** retinal diseases; fetal ischemia; oxygen-glucose deprivation and reperfusion; human retinal organoids; retinal ganglion cells

DOI: 10.18240/ijo.2025.08.03

Citation: Yan YH, Li HY, Gao LX, Li W, Zhao LP, Zeng Q, Luo Y, Cui TT, Zang RG, Ye Z, Xi JF, Yue W, Li ZH. Damaging effect of ischemia on the development of retinal organoids derived from human embryonic stem cells. *Int J Ophthalmol* 2025;18(8):1433-1449

INTRODUCTION

Fetal ischemia due to intrauterine distress can lead to serious developmental disorders, called intrauterine distress in the newborn babies. The incidence of intrauterine distress globally is about 10%^[1]. Intrauterine growth retardation, decreased fetal movement and even stillbirth are some of the unfavorable outcomes of intrauterine distress^[2-3], thus, posing a serious threat to fetal development and even

life of the newborn. In recent years, with the widespread adoption of perinatal monitoring, ocular developmental damage in surviving infants has also garnered attention. Data show that approximately 28.29% of infants who survive intrauterine distress exhibit retinal ischemic damage such as postpartum retinal hemorrhage, suggesting that intrauterine distress can impair retinal development^[4]. Although there is currently limited clinical data for evaluation, various ischemic retinal pathologies in adults, such as diabetic retinopathy^[5], glaucoma^[6] and central retinal artery occlusion^[7] have shown irreversible retinal damage. Combined with reports about the sensitivity of embryonic retina to ischemia^[8], it is suggested that the embryonic retina during intrauterine distress may exhibit similar or even more severe visual impairments, increasing the medical burden on families and society. Therefore, clarifying the early retinal ischemic damage and its mechanisms in infants with intrauterine distress is of significant importance.

Due to ethical constraints and the limitations of clinical examination methods such as ultrasound in assessing retinal damage in fetuses, research on fetal retinal ischemic injury necessitates the support of retinal ischemia models^[9-10]. In studies utilizing two-dimensional cell models or animal models, ischemic retinas exhibit detrimental alterations such as thinning of the neural retinal layers, reduction in photoreceptor cells, and increased apoptosis of ganglion cells, ultimately manifesting as significant visual field defects, diminished visual acuity, and even blindness^[11-13]. Although these investigations have systematically explored the damaging effects of ischemia on the retina, the majority of them are based on mature retinal models, which are unsuitable for examining retinal ischemic changes in infants suffering from intrauterine distress. Consequently, there is a need to construct new early-stage retinal ischemia models for further investigations.

In recent years, human retinal organoids (hROs), derived from human embryonic stem cells, have been widely used in constructing retinal disease models^[14], high-throughput drug screening^[15], genetic diagnosis and therapy^[16], and regenerative transplantation^[17]. In terms of modeling, hROs possess a genetic background and cell surface markers that align with those of the human retina. They are capable of replicating the changes in cell marker expression and the processes of cell differentiation and migration that occur during retinal development^[18]. They can effectively compensate for the shortcomings of existing two-dimensional cell models and animal models in simulating human retinal development processes, histological structures, and gene expression. Simultaneously, there have been breakthroughs in recent years in the experimental strategies for constructing ischemia models

using organoids. Researchers have successfully established an *in vitro* stroke model by treated cerebral organoids with oxygen-glucose deprivation and reperfusion (OGD/R), demonstrating that this treatment can induce a neural damage phenotype in the organoids. Compared to the hypoxia^[19] or simple glucose-oxygen deprivation treatment^[20], the OGD/R treatment simulates both the direct ischemic injury and the reperfusion injury that occur during ischemia^[21]. This approach is more suitable for researching the short-term ischemic injury process experienced by surviving fetuses following intrauterine distress. Consequently, the hROs treated with OGD/R may become a novel model for investigating the pathological changes and pathogenesis of early-stage retinal ischemic diseases. In addition to early retinal ischemic injury caused by intrauterine distress, there may also be a self-repair mechanism in the process of retinal development in infants that responds to ischemic damage^[22]. Relevant studies have indicated that the early retina may activate the protein kinase B/mammalian target of rapamycin (AKT/mTOR) pathway by inducing microglial cell differentiation and the secretion of inflammatory factors, thereby promoting the functional development and regenerative repair of human retinal ganglion cells^[23]. Another study also indicates that the increase in hypoxia inducible factor-1 (HIF1 α) during ischemia may mediate the early retina's adaptation to hypoxic environments by regulating angiogenesis and promoting the expression of anti-injury genes, thereby rescuing ischemic retinal damage^[24]. Although these studies suggest the existence of a repair mechanism for ischemic injury in retinal development, the reparative effect has also not yet been validated by *in vitro* developmental models. The early retinal ischemia model constructed with hROs may be able to recapitulate this damage repair process.

This study employs embryonic stem cells to induce hROs and establishes an early retinal ischemic model through OGD/R treatment, simulating the process of fetal retinal ischemia to validate the detrimental effects of intrauterine distress on the fetal retina. Furthermore, the study maintains hROs treated with OGD/R at different stages until day 60 to investigate the self-repair capacity of retinal development and its correlation with the timing of ischemic events. This provides a basis for predicting the long-term retinal prognosis of children with intrauterine distress based on the onset time.

MATERIALS AND METHODS

Ethical Approval The embryonic stem cell of line 9 used in this study were purchased from the WiCell Research Institute in the United States. As a commercially available cell line, they are inapplicable for ethical approval. All experiments involving human cells were conducted in accordance with the principles of Declaration of Helsinki.

Culturing of Human Embryonic Stem Cells The protocol of stem cell species selection and culture was provided by our team^[25]. Briefly, WA09 human embryonic stem cells were obtained from the Wicell Research Institute and used a feeder-free culture protocol to culture. Briefly, Matrigel (Corning, Teterboro, NJ, USA) was diluted to a 1% volume concentration with Dulbecco's modified eagle medium/nutrient mixture F-12 (DMEM/F-12) medium (Gibco). Subsequently, 1% Matrigel was added to germ and mycoplasma-free 6-well plates (Thermo, Waltham, MA, USA) at a volume of 1 mL per well and incubated at 37°C for 45min to allow gel formation. Following this, human embryonic stem cells were inoculated at the ratio of 1:50 into 6-well plate which was pre-coated with 1% Matrigel and filled with 3 mL of mTeSR Plus medium (STEMCELL Technologies, Vancouver, Canada) per well. Then, 3 mL of fresh medium was replaced in each well every day. Passage of cells was performed when the cell density reached 80%. Following digestion with 0.5 mmol/L ethylene diamine tetraacetic acid (EDTA, pH=8.0, Biosharp, Hefei, Anhui Province, China), the digestion process was terminated by adding three volumes of mTeSR Plus medium, and the cell suspension was collected for centrifugation and resuspension. Subsequently, the cells were seeded at a ratio of 1:50-1:100 into a 6-well plate covered with 1% Matrigel and 3 mL of mTeSR Plus medium each well.

Immunofluorescence Staining of Human Embryonic Stem Cells The experimental protocol for cell immunofluorescence staining was based on earlier reported work^[25]. Before the staining began, 4% paraformaldehyde (PFA, Servicebio, Wuhan, Hubei, China) was used to fix cells for 30min at room temperature on day 4. After wash off the PFA, 0.2% Triton X-100 and 10% donkey serum were used in turn and incubate 30min each time at room temperature. Then, the following primary antibodies were diluted with 10% donkey serum at the specified ratio to prepare the primary antibody dilution, which was subsequently used to co-incubate the cells sealed with the antigen overnight at 4°C: rabbit anti-NANOG homeobox protein (NANOG; 1:200, Abcam, UK), rabbit anti-octamer binding transcription factor 4 (OCT4; 1:250, Abcam) and rabbit anti-sex determining region Y box protein 2 (SOX2; 1:200, Abcam). On the following day, cells were incubated for 1h with AlexaFluor-568-conjugated secondary antibody (1:400, Thermo) in Dulbecco's phosphate buffered saline (DPBS; Gibco, Grand Island, NY, USA) by avoiding light at room temperature. Later, cells were washed off with DPBS for three times (5min at a time) and counterstained with 4',6-diamidino-2-phenylindole (DAPI, 1:500, Sigma, Saint Louis, MO, USA) for 10min at room temperature. Finally, images were captured by Zeiss Axio Imager Z2 microscope (Zeiss, Oberkochen, Germany) with TissueFAXS software (TissueGnostics GmbH,

Vienna, Austria) at 200× magnification, and prepared using Image J software (Version 2.14.0, NIH, Bethesda, MD, USA) for Windows.

Flow Cytometry of Human Embryonic Stem Cells The experimental protocol of flow cytometry was based on past research in our laboratory^[25]. Human embryonic stem cells were digested the clone into a single cell with the Accutase (STEMCELL Technology), which was then incubated with Alexa Fluor 647 mouse anti-stage specific embryonic antigen 4 (SSEA4) monoclonal antibody (BD Biosciences, Franklin Lake, NJ, USA, 2 µL per test) and anti-TRA-1-60-PE antibody (Miltenyi Biotec, Bergisch Gladbach, Germany, 1 µL per test) for 30min at 4°C without light on day 4. Labelled cells suspension was washed twice with DPBS and filtrated into flat 96-well plate before detection. Flow cytometry was carried out on Luminex Guava easyCyte (Millipore, Billerica, MA, USA), and data analysis was performed on FLOWJO software (Version 10.4, Ashland, OR, USA).

Alkaline Phosphatase Staining of Human Embryonic Stem Cells The experimental protocol for alkaline phosphatase staining of embryonic stem cells was based on past research in our laboratory^[25]. After washing off the culture medium with DPBS, human embryonic stem cells were fixed for 30min by 4% PFA at room temperature, and then PFA was cleaned off. Subsequently, the 5-bromo-4-chloro-3-indolyl phosphate/tetranitroblue tetrazolium chloride alkaline phosphatase (BCIP/NBT AP) Color Development Kit (Beyotime, Shanghai, China) was added and cells were kept in dark place for 10min at room temperature. After incubation, the staining was terminated with DPBS and the cells were transferred for Nikon fluorescence microscopy (Ti S, Nikon Corporation, Tokyo, Japan). Images were equipped with NIS-ELEMENTS software (Version D4.30.00, Nikon Corporation, Tokyo, Japan).

Three-dimensional Culturing for Inducing Human Retinal Organoids hROs were produced according to the culture protocol of our previous study^[25-26]. In brief, human embryonic stem cells was dissociated with Accutase containing 20 µmol/L Y-27632 and 1.2×10^4 cells into each hole of the V-bottomed 96-well conical plate (PrimeSurface; Sumitomo Bakelite, Tokyo, Japan) with 100 µL growth factor-free chemically defined medium (gfCDM) supplemented with 10% knock-out serum replacement (Gibco), 20 µmol/L Y-27632 (Selleck Chemicals, Houston, USA), 3 µmol/L IWR1-endo (Selleck Chemicals), 10 µmol/L SB-431542 (Selleck Chemicals) and 100 nmol/L LDN-193189 (Selleck Chemicals). The gfCDM contained 45% Iscove's modified Dulbecco's medium-GlutaMAX (Gibco), 45% Ham's F12-GlutaMAX (Gibco), 1% chemically defined lipid concentrate (Gibco) and monothioglycerol (450 mmol/L, Sigma). It was defined as day 0 after cell implantation. On day 6, the

medium was replaced with fresh gfCDM containing 1.5 nmol/L (55 ng/mL) recombinant bone morphogenetic protein 4 (BMP4, R&D, Minneapolis, MN, USA). Subsequently, half of the medium was updated every 3d. On day 18, embryonic bodies were transferred into the neural retina differentiation medium (NRDM). The NRDM consists of DMEM/F12-glutamax (Gibco), 1% N-2 supplement (Gibco), 10% fetal bovine serum (Gibco), 0.5 μ mol/L retinoic acid (Sigma) and 0.1 mmol/L taurine (Sigma). The fresh culture medium was updated every 3d. These induction experiments were repeated at least three times on different passages of human embryonic stem cells to ensure reproducibility and reliability.

Oxygen-Glucose Deprivation and Reperfusion Treatment

OGD/R treatment followed the protocol of previous studies with some modifications^[27-29]. The hROs on the day 18 or day 30 were transferred to a low-cell adhesion plate with 1.5 mL low-glucose medium and incubated in a hypoxia incubator (1% O₂, 5% CO₂). The low-glucose medium included glucose-free Dulbecco's modified Eagle's medium (Gibco), F12-glutamax (Gibco), 1% retinoic acid (Gibco), 10% fetal bovine serum (Gibco), 0.5 μ mol/L retinoic acid (Sigma) and 0.1 mmol/L taurine (Sigma). After 4h of incubation, the culture medium was restored to NRDM and further incubated for 20h in normal cell incubator (21% O₂, 5% CO₂). The corresponding control group maintained the normal induction protocol for culture. The hROs at both treatment times were maintained until day 60, and Samples were collected after day 18 and day 30 treatment and day 60.

Paraffin Embedding, Preparation and Dyeing of Paraffin Sections

The preparation of paraffin sections was similar to our earlier study^[25]. After randomly collecting three samples from each group per experiment ($n=9$ from three experiments), hROs were fixed into 4% PFA for 12h and progressive dehydrated with a graded series of ethanol and xylene and sealed in paraffin wax (The fixed organoids were sequentially dehydrated in 50%, 60%, and 70% ethanol for 15min each, followed by sequential transfer into 80%, 90%, 95%, 100% I, and 100% II ethanol, with each concentration maintained for 10min. Then, the organoids were treated with a 1:1 xylene-anhydrous ethanol solution for 10min and subsequently immersed in pure xylene twice, each for 10min. Finally, the organoids are transferred to melted paraffin wax for 20min. Then paraffin samples were then cut into several 5 μ m thick slices until tissues disappeared by using the paraffin microtome (Leica, Weztlar, Germany). The slices were dried and stored in a cool place.

For the staining of paraffin sections, slices across the long axis of hROs were selected. Then, sections were initially immersed in pure xylene twice, each for a duration of 15min. Subsequently, they were transferred through a graded series

of ethanol solutions (100%, 90%, 70%, and 50%) for 10min each, followed by a final rinse in distilled water for 10min. Following the completion of the aforementioned dewaxing and rehydration processes, immunofluorescence staining was subsequently initiated. Firstly, these slices were incubated for 30min with 0.2% Triton X-100 and 10% donkey in turn at 20°C. Later, these slices were then incubated with the following primary antibodies dissolved in 10% donkey serum: anti-Ki67 (1:200; Abcam), anti-paired box gene 6 (PAX6) (1:250; Abcam), anti-SOX2 (1:200; Abcam), anti-CHX10 (1:200; Santa Cruz, Dallas, TX, USA), anti- β tubulin III (TUJ1, 1:250; Beyotime), anti-brain specific homeobox/POU domain protein 3 (BRN3; 1:50; Santa Cruz) and anti- neuroepithelial stem cell protein (NESTIN; 1:200; Sigma) overnight at 4°C. Then, goat anti-mouse Alexa-Fluor-568 (Life technologies, 1:400) or goat anti-rabbit Alexa-Fluor-488 (Life technologies, A11011, 1:400) secondary antibodies, diluted in DPBS, were used to incubate for 1h in 25°C (1:400; Thermo). After being counterstained with DAPI (1:500, Sigma) and sealed, the images were captured at 200 \times magnification with a confocal microscope (Dargonfly 200, ANDOR Technology, Belfast, Northern Ireland).

Fluorescent Cell Counting The whole counting method was based on past research by our team^[25]. At least nine comparable sections from three different batches of the hROs were selected and counted ($n=9$ from three experiments). Cell numbers were determined by Image J software (NIH). Three 200 μ m \times 200 μ m rectangular areas were randomly chosen from each section, and the rate of labeled cells and DAPI-stained cells in the area were counted. Specifically, only retinal cells located in neural retina were counted, cells in the central necrotic area were excluded.

Flow Cytometry of Human Retinal Organoids The flow cytometry analysis was based on our earlier study^[25]. Five organoids from three different batches of the hROs in each group ($n=15$ from three experiments) were randomly collected and digested by Accutase (Gibco) containing DNase I (Sigma) and collagenase D (Sigma) on day 18. And 1×10^4 cells (one test) were taken to co-incubate with annexin protein V (Annexin V)-FITC and 7-aminoactinomycin D (7AAD; Elabscience Biotechnology, Wuhan, Hubei Province, China) at 4°C for 30min. All flow cytometry were performed on Luminex Guava easyCyte (Millipore), and the data were analyzed by FLOWJO software (Version 10.4).

RNA Extraction and Real-time Quantitative Polymerase Chain Reaction The protocol was derived from past research in our laboratory^[25]. Five organoids from three batches were selected from each group ($n=15$ from three experiments) and the TRIzol reagent (Invitrogen, Carlsbsd, CA, USA) was used to extract RNA. The RNA concentrations were mixed with

Table 1 Primer sequences used for RT-qPCR

Gene symbol	Forward primer sequence (5'-3')	Reverse primer sequence (5'-3')
<i>Ki67</i>	GCAAGCACTTTGGAGAGCAA	ACACACATTGTCCTCAGCCTTC
<i>PAX6</i>	ACCCACCACACCGGTTTCC	GGGCAGCATGCAGGAGTATGA
<i>SOX2</i>	TGGACAGTTACGCGCACAT	GCGAGCCGTTTCATGTAGGT
<i>CHX10</i>	GAAGACAGGATACAGGTCTGGTT	GCCATCCTGGCTGACTTGA
<i>ATOH7</i>	CGTCTCCACTGTGAGCACTTCG	TGGAAGCCGAAGAGTCTCTGGC
<i>TUBB3</i>	CCTGACAATTTTCATCTTTGGTCAGA	CATGATGCGGTCGGGATACT
<i>POU4F1</i>	AGGGTCAGGGACAGAGGAAT	CACTGTGGAGCAGTAGGTGG
<i>GAPDH</i>	ATTGCCCTCAACGACCACT	ATGAGGTCCACCACCTGT

RT-qPCR: Real-time quantitative polymerase chain reaction.

reverse transcription mix (Toyobo, Osaka, Japan) to reverse to cDNA. When performing real-time quantitative polymerase chain reaction (RT-qPCR), the expression of the target gene was detected by using Toyobo PCR Master Mix (Toyobo) on the CFX Manager system (version 3.1, Bio-Rad Laboratories, Hercules, CA, USA) according to the manufacturer's instructions. The primers of the target genes are summarized in Table 1.

Protein Extraction and Western Blot Assay Five hROs from three batches of each group ($n=15$ from three experiments) were collected to extract proteins. According to the manufacturer's instructions, RIPA lysis buffer (CW BIO, Taizhou, Jiangsu, China) were mixed with protease inhibitors (Selleck Chemicals) and phosphatase inhibitors (Bimake, New York, USA) to extract proteins. The concentration of extracted protein from each group was measured by BCA protein assay kit (Thermo) and balanced by using RIPA lysis buffer. Then the laemmli sample buffer (Bio-rad, 1:3) was mixed in and denatured for 5min at 95°C.

For Western blot (WB), proteins (10 μ L per well) were separated on a 12% sodium dodecyl sulfate polyacrylamide gel (SDS-PAGE; Tsingke Biotech, Beijing, China) and transferred to polyvinylidene fluoride (PVDF; Millipore) membranes. After blocking with 5% skim milk for 1h at 37°C, the membranes were incubated with primary antibodies, including anti-TUJ1 (Beyotime, 1:2000), anti-proliferating cell nuclear antigen (PCNA; Santa Cruz, 1:2000), anti-human protein atonal homolog 7 (ATOH7; Thermo, 1:2000) and anti-glyceraldehyde-3-phosphate dehydrogenase (GAPDH) (ABclonal Technology, Wuhan, Hubei, China) overnight at 4°C. Then the membrane was washed thrice with buffer and incubated with goat anti-rabbit and anti-mouse secondary antibody (Invitrogen, 1:2000) for 1h at room temperature. Before capturing images by Amersham Imager 680 (GE Healthcare, Chicago, USA), Chemiluminescent HRP Substrate (Millipore) was incubated with the membrane. Relative protein expression levels were quantified using Image J software (NIH) with GAPDH as control.

Statistical Analysis For statistical analysis, the data were analyzed by Statistical Product and Service Solutions software V22.0 (SPSS, Chicago, IL, USA) and Graphpad Prism (Version 9.5.0, San Diego, CA, USA). The comparison of data between two independent groups employs the unpaired two-tailed t-test as the statistical strategy. All data are expressed as the mean standard deviation. The significance level was set at $P<0.05$.

RESULTS

Construction of Retinal Development Model Based on Retinal Organoids Derived from Human Embryonic Stem Cells

In order to induce hROs, human embryonic stem cells were identified and used as seed cells. Human embryonic stem cells, grown in feeder-free culture environment, displayed typical clone-like growth (Figure 1A). SSEA4-positive/TRA-1-60-positive stem cells accounted for 93.7% of all human embryonic stem cells (Figure 1B). Human embryonic stem cells expressed stem cell markers NANOG, OCT4 and SOX2 (Figure 1C-1E). And human embryonic stem cells proliferated vigorously (Figure 1F). This indicates that human embryonic stem cells exhibited the characteristics of embryonic stem cells, so that it could be used as seed cells to induce hROs.

Under the microscopic light field, hROs were observed to form continuous semitransparent neural epithelium on day 18, and neuroepithelium then thickened by day 60 (Figure 2A). Immunofluorescence staining revealed that the original SOX2-positive neural retinal lamellar morphology formed in hROs contained CHX10- and PAX6-positive retinal progenitor cells on day 18 (Figure 2B, 2C). TUJ1-positive/BRN3-positive immature retinal ganglion cells also started to emerge on day 18, and its axons migrated along the skeleton of NESTIN-positive neural fibers (Figure 2D, 2E). On day 30, the neural retina layer thickened, and PAX6-positive retinal progenitor cells were separated from SOX2-positive neural stem cells (Figure 2F, 2G). Immature retinal ganglion cells also migrated inward to form the retinal ganglion cell layer (Figure 2H, 2I). After that, hROs continued to thicken until day 60 (Figure 2J-2M). These results showed that the hROs imitated the physiological

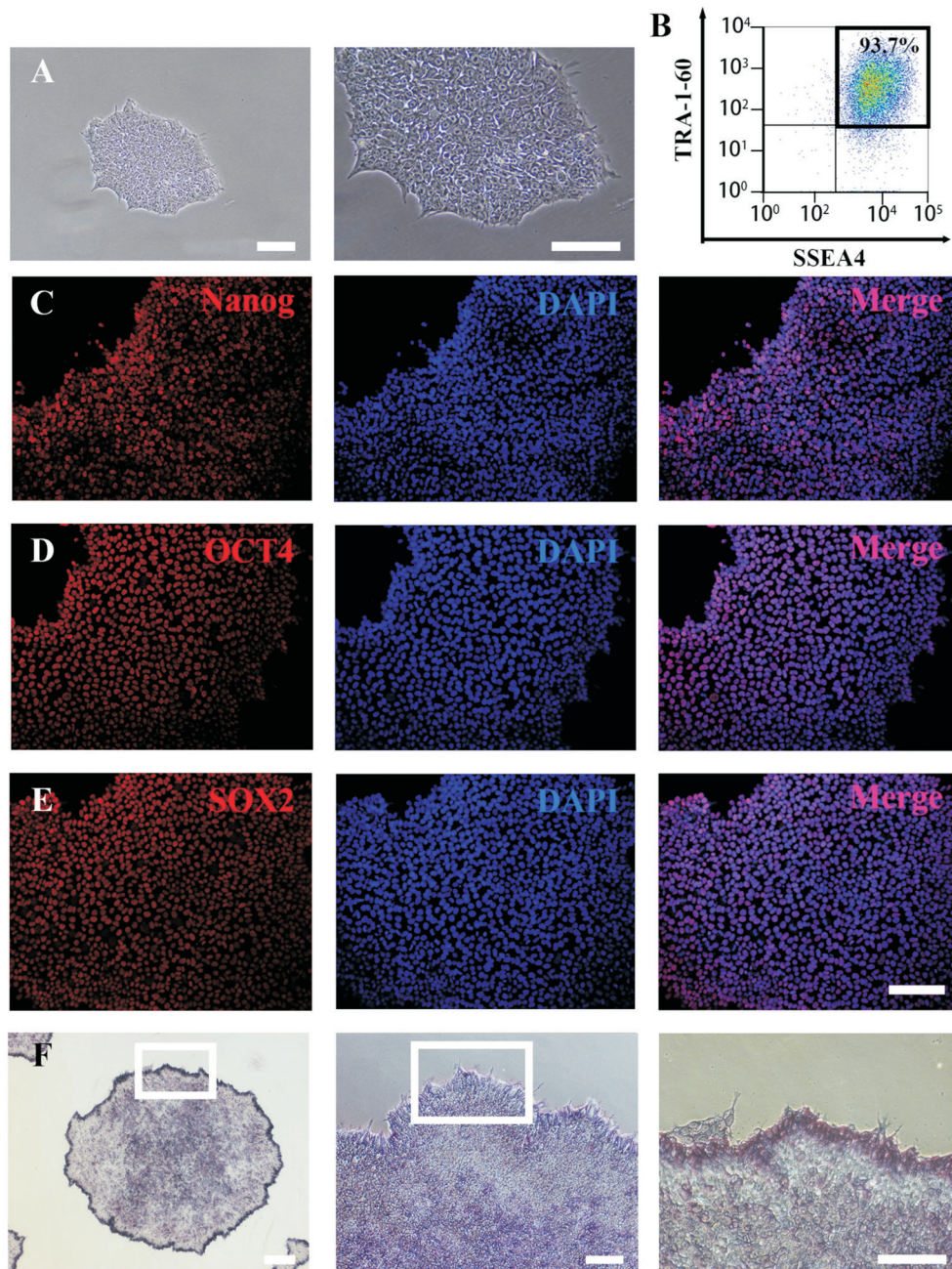


Figure 1 H9 embryonic stem cells had stem cell stemness A: Human embryonic stem cells had typical adherent round shape and clone-like growth under the bright field. B: The expression of pluripotent stem cell surface markers SSEA4 and TRA-1-60 in human embryonic stem cells by flow cytometry. C-E: Representative immunofluorescent images of human embryonic stem cells stained stemness markers NANOG (C), OCT4 (D) and SOX2 (E). The magnification was 200 \times , and the nuclei were stained with DAPI (blue). F: Representative alkaline phosphatase-stained images of human embryonic stem cells at 4 \times , 10 \times , and 20 \times magnification. Scale bar: 100 μ m. SSEA4 and TRA-1-60: Pluripotent stem cell surface markers. NANOG: Stemness markers. OCT4: Octamer binding transcription factor 4; SOX2: Sex determining region Y box protein 2; DAPI: 4',6-diamidino-2-phenylindole.

development process of neural retina and could be used as an *in vitro* retinal development model for the follow-up study.

Damaging Effect of Oxygen-glucose Deprivation and Reperfusion on Retinal Cell Proliferation The hROs needed to undergo complex environmental changes to complete the OGD/R treatment process on day 18 or day 30 (Figure 3A). After OGD/R treatment on day 18, the proportion of Ki67-positive

proliferating cells decreased under controlled conditions ($P=0.0097$; Figure 3B-3D), and the expression of proliferating protein Ki67 decreased (Figure 3E). Compared with control group, the transcription level of proliferation marker mRNA decreased ($P=0.0005$; Figure 3F). Above results indicated that the proliferative ability of retinal cells was impaired by OGD/R treatment. In addition, the proportion of early apoptotic cells

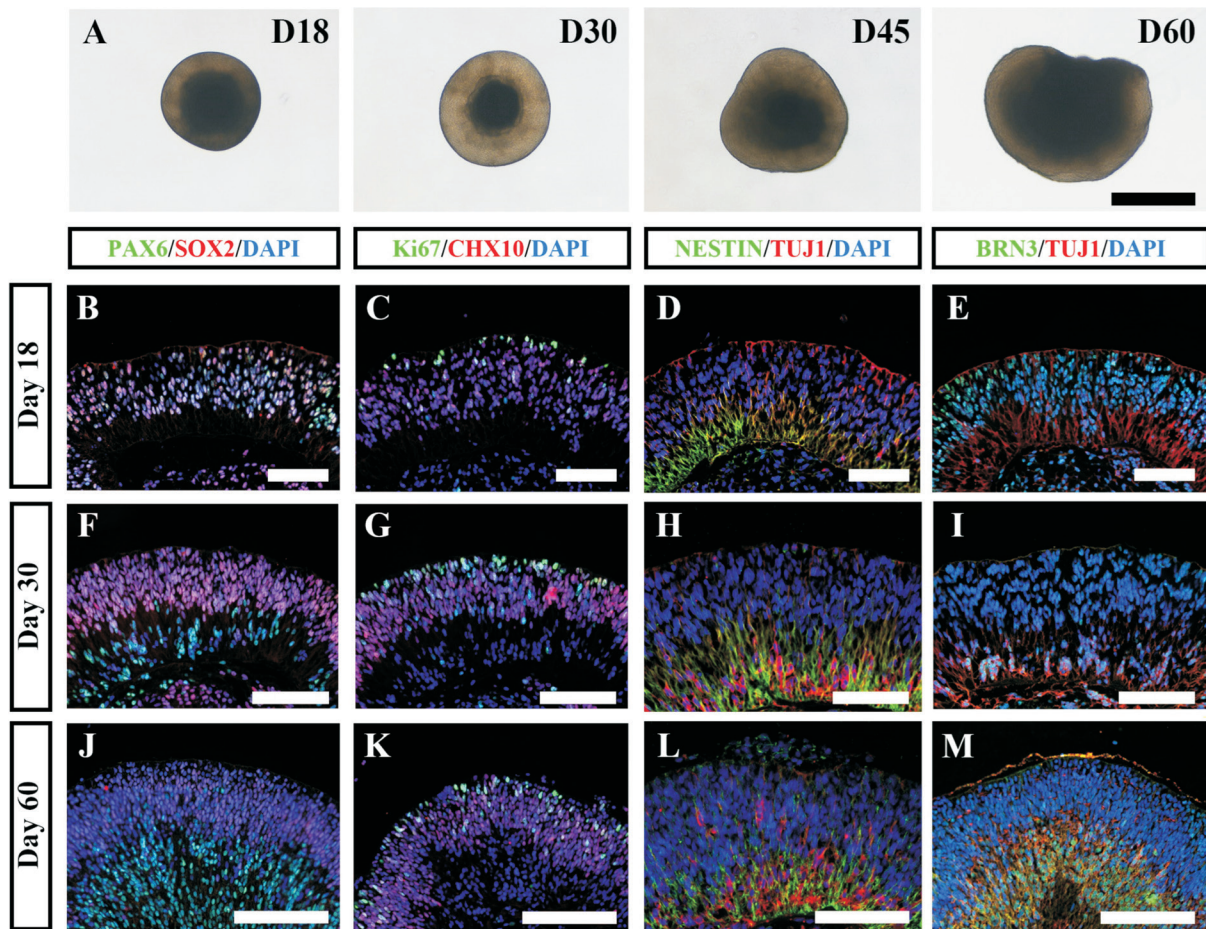


Figure 2 The formation and neurogenesis of hROs A: The representative microscopic images of hROs were captured on day 18, day 30, day 45 and day 60. The magnification was 100 \times . Scale bar: 500 μ m. B-M: Representatives immunofluorescence staining images of hROs on day 18 (B-E), day 30 (F-I) and day 60 (J-M). Representative retinal cells were stained including Ki67-positive proliferating cells, SOX2-positive neural stem cells, CHX10- and PAX6-positive retinal progenitor cells, NESTIN-positive neural fibers and TUJ1-/BRN3-positive retinal ganglion cells. Cell nuclei were stained with DAPI (blue). Scale bar: 100 μ m. PAX6: Paired box gene 6; SOX2: Sex determining region Y box protein 2; Ki67: Proliferating cellular marker; CHX10: Retinal progenitor cellular marker; NESTIN: Neuroepithelial stem cell protein; TUJ1: β tubulin III; BRN3: Brain specific homeobox/POU domain protein 3; DAPI: 4',6-diamidino-2-phenylindole.

relatively increased in OGD/R treatment group ($P=0.0448$; Figure 3G, 3H).

In addition, on evaluating the change in organoid proliferative ability after OGD/R exposure on day 30, the representative immunofluorescence image showed, the Ki67-positive cells relatively decreased in the same size visual field after treatment. In the context of comparison, the proportion of proliferating cells in hROs decreased after treatment ($P=0.0418$; Figure 4A, 4B). Overall, OGD/R treatment weakened the proliferation ability of hROs.

Damaging Effect of Oxygen-Glucose Deprivation Reperfusion on the Development of Retinal Neural Stem Cells and Retinal Progenitor Cells In order to explore the effects of ischemia on retinal neurogenesis, changes of stem/progenitor cells were recorded after OGD/R treatment on day 18. Immunofluorescence staining suggested a decrease in the ratio of SOX2-positive retinal neural stem cells and CHX10-

positive retinal progenitor cells, and an increase of PAX6-positive retinal progenitor cells in CHX10-positive retinal progenitor cells (Figure 5A). Compared with the control group, the proportion of SOX2-positive retinal neural stem cells decreased after treatment ($P=0.0072$; Figure 5B). And similar situation occurred to CHX10-positive retinal progenitor cells under control conditions ($P=0.0101$; Figure 5B). However, the ration of PAX6-positive retinal progenitor cells in CHX10-positive retinal progenitor cells was higher compared to the control group after treatment ($P=0.0263$; Figure 5B). The change of SOX2, CHX10 and PAX6 mRNA transcription level is consistent with the change of cellular proportion ($P=0.0163$, 0.0158 and 0.0489, respectively). These experimental results showed that OGD/R treatment can damage the retinal stem and progenitor cells and induce the differentiation of PAX6-positive retinal progenitor cells, thus, abolishing the original trajectory of cellular development.

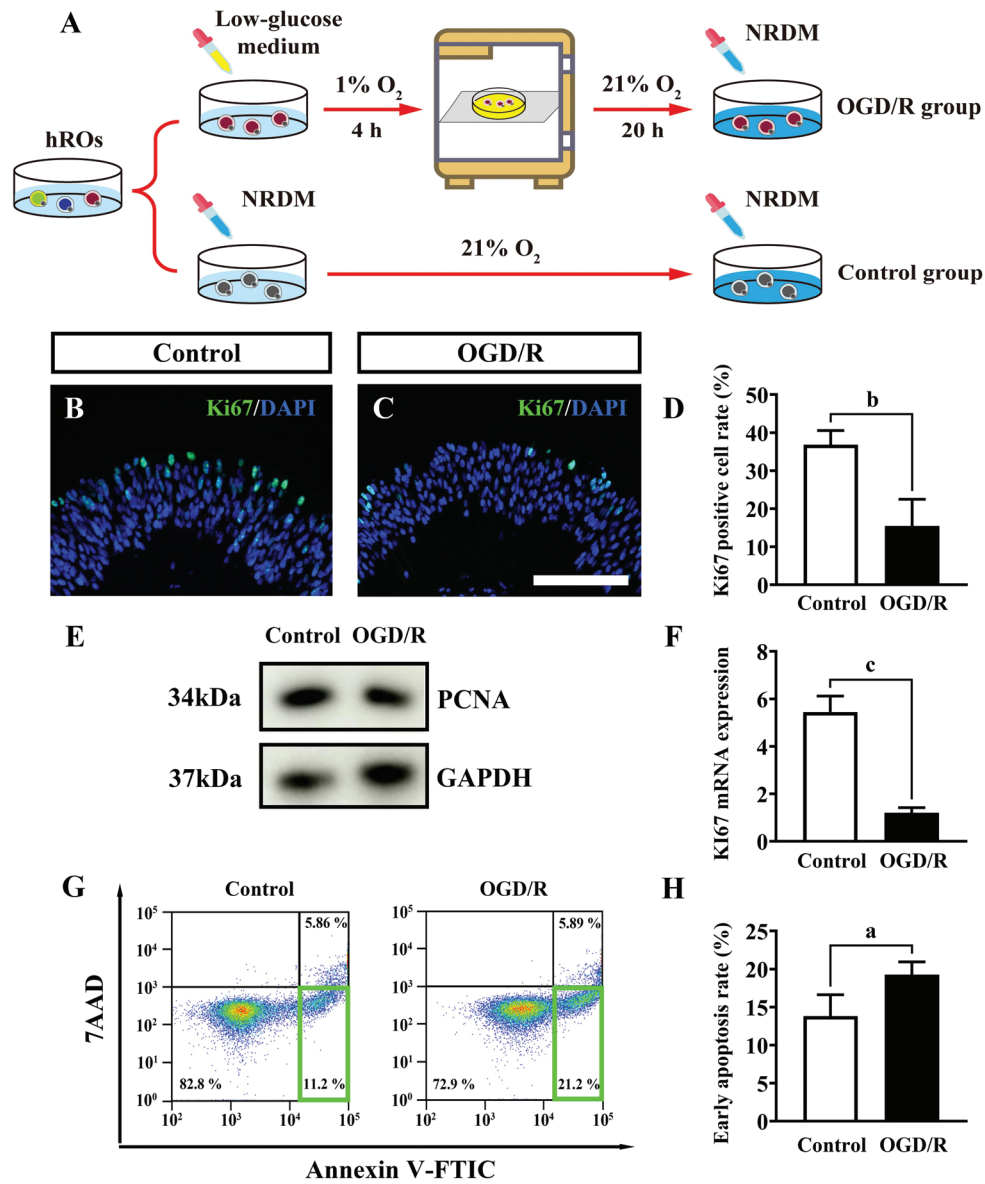


Figure 3 OGD/R treatment damage the proliferative ability of retinal cells on day 18 A: Schematic diagram of the OGD/R treatment. B-C: Representative immunofluorescent images showed the proliferative marker positive cells in neural retina before (B) and after OGD/R treatment (C) at day 18. Nuclei were stained with DAPI (blue). Scale bar: 100 μ m. D: Comparative analysis of numbers of Ki67-positive retinal proliferative cells by unpaired two-tailed *t*-test ($n=15$ from three experiments). Error bars represent standard deviations. E: Representative images of WB stained for proliferative protein PCNA and housekeeping protein GAPDH on day 18. F: Statistical graph of the relative expression levels of Ki67 mRNA, normalised by GAPDH ($n=15$ from three experiments). Error bars represent standard deviations. G: Representative images of flow cytometry showed the increased apoptosis of hROs cells after OGD/R treatment on day 18. H: Comparative analysis of early apoptotic cells by unpaired two-tailed *t*-test ($n=15$ from three experiments). Error bars represent standard deviations. ^a $P<0.05$; ^b $P<0.01$; ^c $P<0.001$. OGD/R: Oxygen-glucose deprivation and reperfusion; hROs: Human retinal organoids; WB: Western blot; DAPI: 4',6-diamidino-2-phenylindole; NRDM: Neural retina differentiation medium; PCNA: Proliferating cell nuclear antigen; GAPDH: Glyceraldehyde-3-phosphate dehydrogenase; 7AAD: 7-aminoactinomycin D; Annexin V: Annexin protein V.

Furthermore, we also evaluated the effect of OGD/R exposure on day 30 in hROs stem/progenitor cells. After OGD/R treatment on day 30, the thickened PAX6-positive retinal progenitor cell layer was exposed by immunofluorescence staining, and the number of the PAX6-positive retinal progenitor cells increased ($P=0.0094$; Figure 4B). The declined transcriptional level of CHX10-positive retinal

progenitor cells and the increased transcriptional level of PAX6-positive retinal progenitor cells in hROs on day 30 revealed the tendency of differentiation of CHX10-positive cells into PAX6-positive cells induced by OGD/R treatment ($P=0.0421$ and 0.0466 , respectively; Figure 4D). Above results were similar to those in day 18, which indicated that OGD/R treatment could damage retinal stem/progenitor

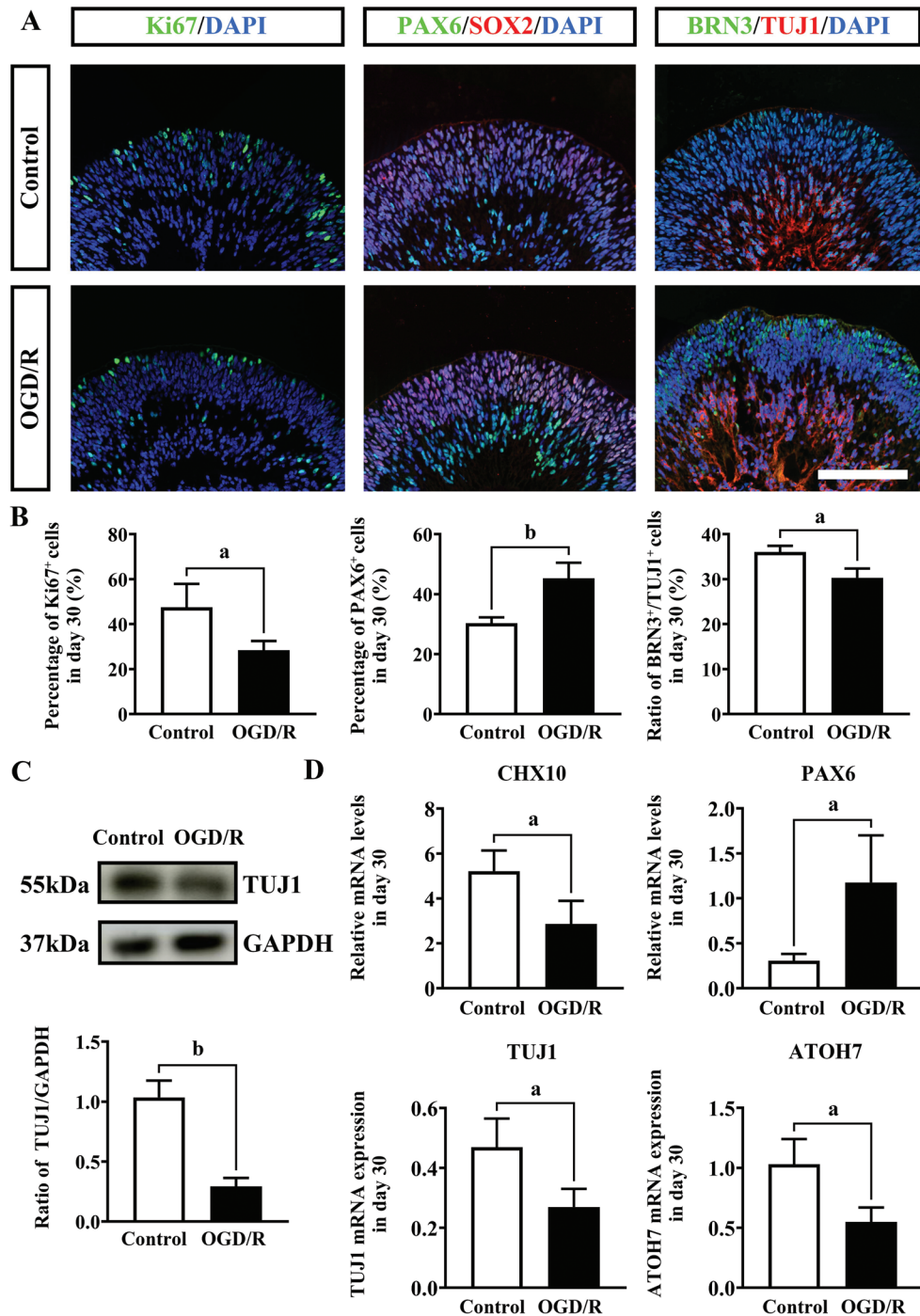


Figure 4 OGD/R treatment on day 30 damaged the process of retinal development A: Representative immunofluorescent images stained for Ki67, PAX6, SOX2, TUJ1, BRN3 in neural retina at 200× magnification on day 30. Nuclei were counterstained with DAPI (blue). Ki67: Retinal proliferating cells. CHX10 and PAX6: Retinal progenitor cells. TUJ1 and BRN3: Retinal ganglion cells. Scale bar: 100 μm. B: Compared analysis of the proportion of the Ki67-positive, PAX6-positive and BRN3-positive cells in two groups after OGD/R treatment on day 30 by unpaired two-tailed *t*-test ($n=9$ from three experiments). Error bars represent standard deviations. C: Representative images of WB stained for retinal ganglion cell marker protein TUJ1 on day 30, and compared analysis of retinal ganglion cell marker protein by unpaired two-tailed *t*-test, normalised by GAPDH ($n=15$ from three experiments). Error bars represent standard deviations. D: Statistical graph of relative mRNA levels of Ki67, CHX10, PAX6, TUJ1 and ATOH7 on day 30, normalised by GAPDH ($n=15$ from three experiments). Error bars represent standard deviations. ^a $P<0.05$; ^b $P<0.01$. OGD/R: Oxygen-glucose deprivation and reperfusion; WB: Western blot; Ki67: Proliferating cellular marker; PAX6: Paired box gene 6; SOX2: Sex determining region Y box protein 2; CHX10: Retinal progenitor cellular marker; TUJ1: β tubulin III; BRN3: Brain specific homeobox/POU domain protein 3; ATOH7: Human protein atonal homolog 7; DAPI: 4',6-diamidino-2-phenylindole; GAPDH: Glyceraldehyde-3-phosphate dehydrogenase.

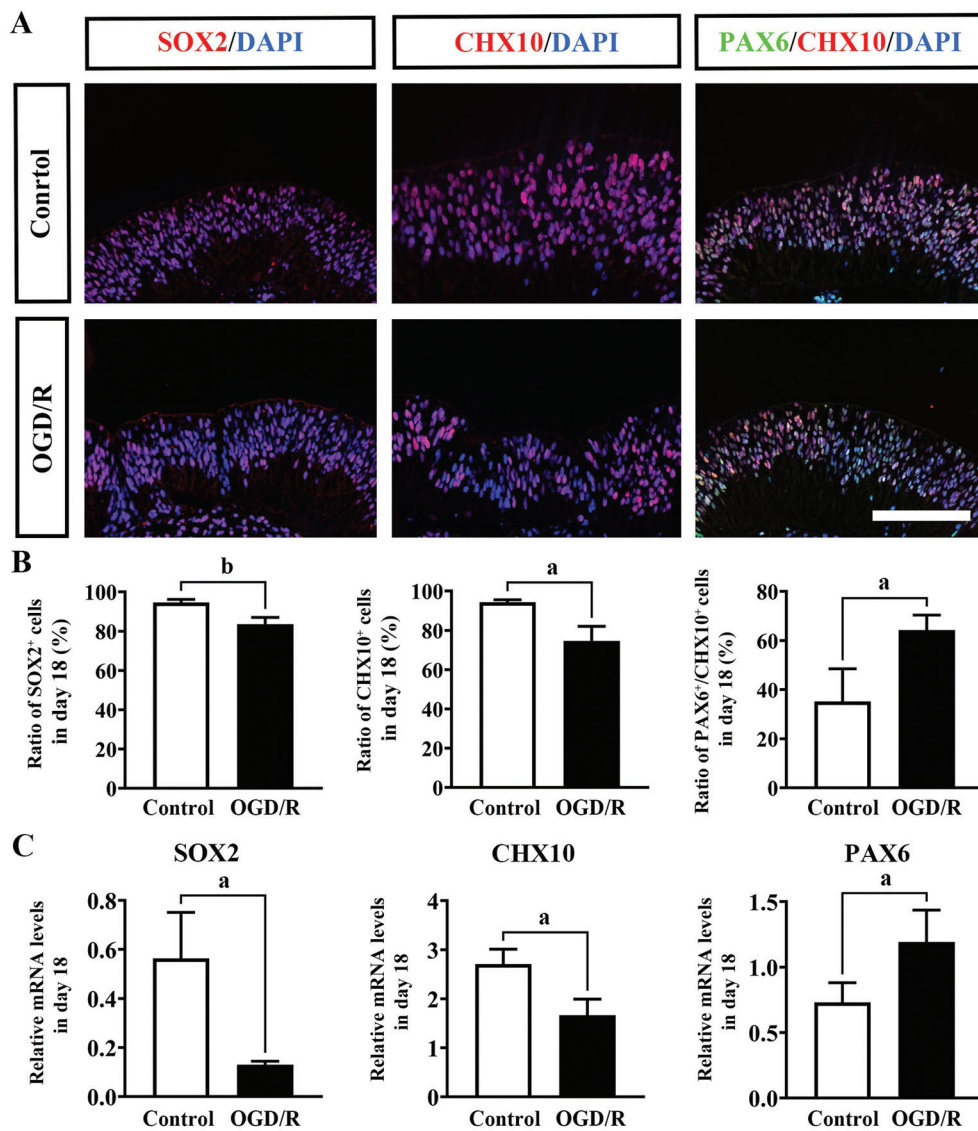


Figure 5 Retinal stem/progenitor cell development on day 18 was injured by OGD/R treatment A: Representative immunofluorescent images showed the staining for SOX2-positive, CHX10-positive and PAX6-positive cells on day 18. Nuclei were stained with DAPI. CHX10 and PAX6: retinal progenitor cells. Scale bar: 100 μ m. B: The proportion of the SOX2-positive and CHX10-positive cells decreased, but PAX6-positive cells increased after OGD/R treatment at day 18 ($n=9$ from three experiments). Error bars represent standard deviations. C: The relative mRNA levels of SOX2, CHX10 and PAX6, normalised by GAPDH ($n=15$ from three experiments). Error bars represent standard deviations. ^a $P<0.05$; ^b $P<0.01$. OGD/R: Oxygen-glucose deprivation and reperfusion; SOX2: Sex determining region Y box protein 2; CHX10: Retinal progenitor cellular marker. PAX6: Paired box gene 6; DAPI: 4',6-diamidino-2-phenylindole; GAPDH: Glyceraldehyde-3-phosphate dehydrogenase.

cell differentiation and change the cell composition in stem/progenitor cell pool.

Axonal Extension, Migration and Differentiation Inhibition of Retinal Ganglion Cells Induced by Oxygen-Glucose Deprivation and Reperfusion Treatment To identify the effect of ischemia on early retinal ganglion cell development, we observed the changes of several ganglion cell markers before and after OGD/R treatment. Immunofluorescence staining showed that the continuity of TUJ1-positive retinal ganglion cell axonal layer was interrupted after OGD/R treatment on day 18 (Figure 6A). Moreover, the radial migration of TUJ1⁺/BRN3⁺ immature retinal ganglion cells along the NESTIN-positive scaffold declined, and the number of TUJ1-

positive/ATOH7-positive immature retinal ganglion cells migrating to the outer nuclear layer was also decreased (Figure 6A). The subsequent comparative analysis of the number of TUJ1-positive/BRN3-positive and TUJ1-positive/ATOH7-positive retinal ganglion cells verified these staining changes (Figure 5B). The number of TUJ1-positive/BRN3-positive retinal ganglion cells decreased after treatment ($P=0.0122$; Figure 6B). Similarly, the number of TUJ1-positive/ATOH7-positive retinal ganglion cells was lower compared to control ($P=0.0102$; Figure 6B). The expression levels of retinal ganglion cell surfaced marker proteins TUJ1 and nuclear labeled protein ATOH7 were synchronous reduced after OGD/R treatment ($P=0.0137$ and 0.0015 , respectively; Figure

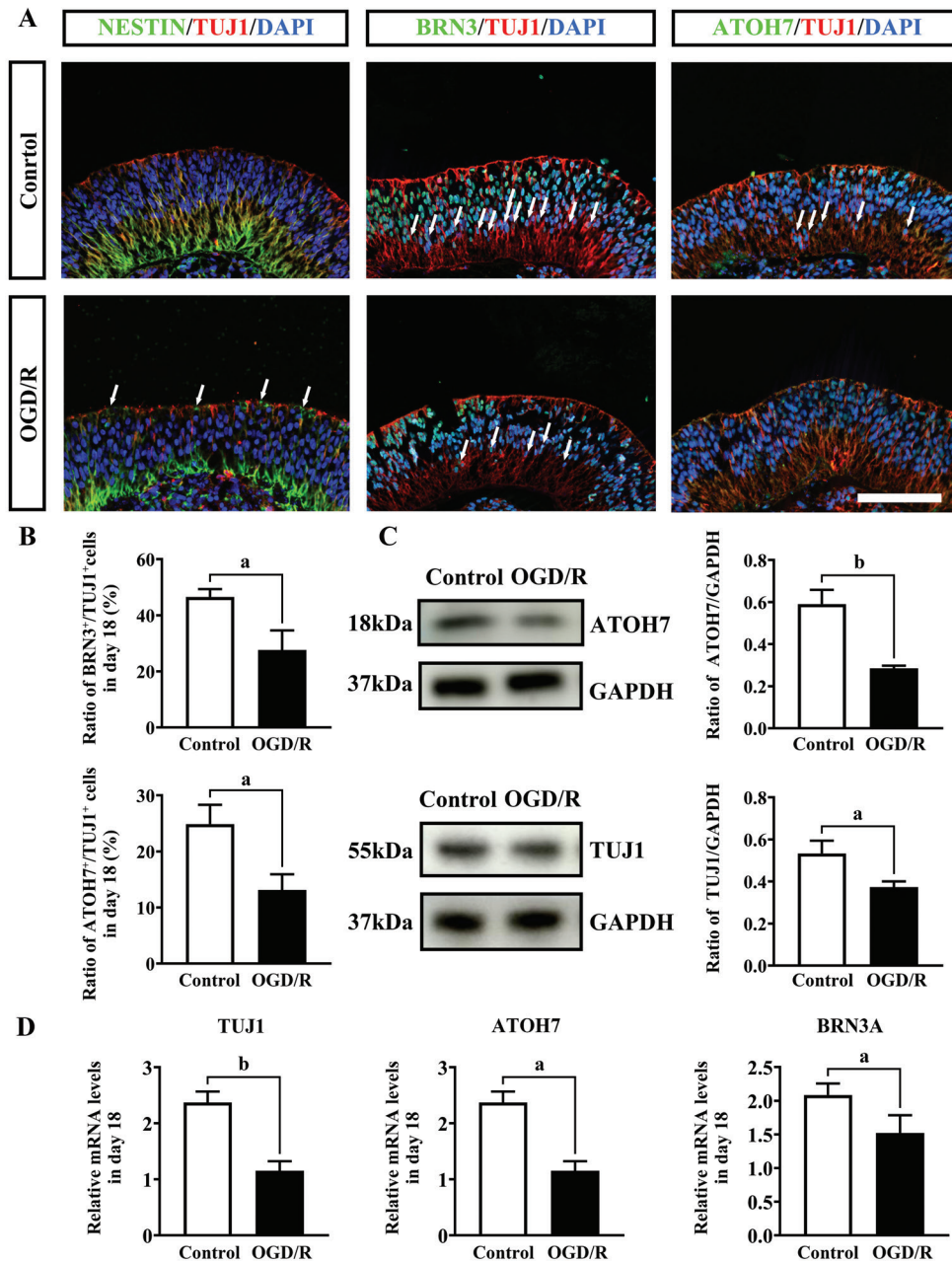


Figure 6 OGD/R treatment disturbed the axonal extension, migration and differentiation of retinal ganglion cells on day 18 A: Representative immunofluorescent images stained for the neural skeleton marker NESTIN, immature retinal ganglion cell axons marker TUJ1, and retinal ganglion cell nuclear marker ATOH7 and BRN3 on day 18. White arrows from left to right represent discontinuity of retinal ganglion cell axons, migrating ATOH-positive retinal ganglion cells and BRN3-positive retinal ganglion cells in different staining. Nuclei were stained with DAPI. Scale bar: 100 μ m. B: Compared analysis of the proportion of the TUJ1-positive/BRN3-positive and TUJ1-positive/ATOH7-positive cells after treatment on day 18 by unpaired two-tailed *t*-test ($n=9$ from three experiments). Error bars represent standard deviations. C: Representative images of WB stained for ATOH7 and TUJ1 on day 18, and compared analysis of retinal ganglion cell marker protein by unpaired two-tailed *t*-test was behind ($n=15$ from three experiments), normalised by housekeeping protein GAPDH. Error bars represent standard deviations. D: The relative mRNA expression of the retinal ganglion cell markers TUJ1, ATOH7 and BRN3A after OGD/R treatment on day 18, normalised by GAPDH ($n=15$ from three experiments). Error bars represent standard deviations. ^a $P<0.05$; ^b $P<0.01$. OGD/R: Oxygen-glucose deprivation and reperfusion; WB: Western blot; NESTIN: Neuroepithelial stem cell protein; TUJ1: β tubulin III; BRN3: Brain specific homeobox/POU domain protein 3; ATOH7: Human protein atonal homolog 7; DAPI: 4',6-diamidino-2-phenylindole; GAPDH: Glyceraldehyde-3-phosphate dehydrogenase.

6C). The mRNA transcription levels of cell markers TUJ1, ATOH7 and BRN3A were also reduced ($P=0.0012$, 0.0341 and 0.0364 , respectively; Figure 6D). All these results suggested that ischemia may induce damage in the immature retinal

ganglion cells in the early stage of development, including hindering retinal ganglion cell axonal extension, migration and differentiation.

Consequently, the relative decline in the proportion of TUJ-

positive/BRN3-positive retinal ganglion cells after treatment on day 30 was observed ($P=0.0161$; Figure 4A, 4B). The decreased expression of ganglion cell markers can also be found when monitoring the development of ganglion cells at the protein and transcriptome level ($P=0.0012$, 0.0386 and 0.0259 , respectively; Figure 4C, 4D). All results suggested that OGD/R has similar damaging effects on retinal ganglion cells at different time interval.

Differential Reversibility of Damage in Human Retinal Organoids Subjected to Oxygen and Glucose Deprivation Reperfusion Treatments at Different Nodes

In order to evaluate the subsequent developmental condition after release from ischemic environment on day 18, various cell markers in hROs of day 60 were recorded. Immunofluorescence staining showed that the CHX10-positive retinal progenitor cell layer was still under the damaged condition, and the number of Ki67-positive retinal proliferating cells was less than that of the control group (Figure 7A). Meanwhile, the PAX6-positive retinal progenitor cell layer was thicker than that of the control group, and the retinal ganglion cell layer also lost its normal structure (Figure 7A). There was relative decrease in the expression of proliferating protein PCNA, and increased expression of retinal ganglion cell markers TUJ1 and ATOH7 (Figure 7B). Comparative analysis of the related mRNA level of Ki67 between the control group and the treatment group showed that the level of proliferation in the day 18 treatment group was relatively low ($P=0.0008$; Figure 7D), which suggested that the proliferation ability of retinal cells had not returned to similar level of the control group. The effect of OGD/R treatment on SOX2-positive neural stem cells was relieved, and the transcriptional level was without significance ($P=0.0717$; Figure 7D). The injury phenotype could still be observed in the CHX10-positive retinal progenitor cell layer, and its transcriptional level was low ($P=0.0035$; Figure 7D). Meanwhile, PAX6-positive retinal progenitor cells maintained a higher level of transcription than that in the control group ($P=0.0017$; Figure 7D). The above results demonstrated that OGD/R treatment on day 18 result in long-term injuries at the level of retinal stem/progenitor cells that could not be completely reversed in the development of hROs. About the change of retinal ganglion cells, the expression level of retinal ganglion cell marker protein TUJ1 and ATOH7 were relatively high (Figure 7C), and the mRNA transcriptional level of TUJ1 and BRN3A was restored ($P=0.0310$ and 0.0008 , respectively; Figure 7D). Although ganglion cell markers have recovered at the transcriptional level and protein expression, the structural damage of ganglion cell layer had not been fully restored.

In addition, we also evaluated the long-term effects of day 30 OGD/R exposure on the development axis of hROs. Under the control condition, the retinal cells on day 30 showed a

recovery of the retinal structure and retinal cell markers during day 60 (Figure 8A). Furthermore, the proliferation protein PCNA and the ganglion cell marker proteins TUJ1 and ATOH7 also returned to the level of the control group (Figure 8B). The transcription level of retinal cell markers recovered and was higher than those of the control group ($P=0.1588$, 0.0042 , 0.3477 and 0.2064 , respectively; Figure 8C). In conclusions, although the OGD/R treatment damaged the development of various retinal cells, it could recover to a certain extent in the follow-up development. And the degree of tissue recovery of the earlier exposure was higher than that of the later exposure.

DISCUSSION

In the present study, an early retinal ischemia model was successfully established in hROs on day 18 and day 30 by treating them with OGD/R. Through this model, we have substantiated that OGD/R treatment induces damage to hROs at either day 18 or day 30. This damage was specifically manifested by the disruption of the normal architecture in the retinal progenitor cell layer and the ganglion cell layer, a reduction in the quantity and marker expression levels of neural stem cells and stem/progenitor cells within the retina, an increase in PAX6-positive progenitor cells, as well as axonal injury and a decrease in the number of ganglion cells. Furthermore, we observed that when hROs were maintained until day 60, the damage induced by OGD/R could be self-repaired. However, the extent of recovery varied among organoids depending on the specific stage at which they underwent OGD/R treatment. Apart from the recovery of ganglion cell marker damage, other OGD/R injuries on day 18 showed no signs of recovery by day 60. In contrast, the OGD/R injury inflicted on day 30 was completely recovered by day 60, with both the structure of the neural retina and the expression of cellular markers returning to normal. These results provided pathological evidence of retinal involvement in intrauterine distress, validated the existence of a self-repair mechanism during retinal development, and suggested a potential method for assessing the extent of self-repair in early retinal ischemia based on the timing of ischemic occurrence.

The findings of this study indicate that ischemia results in a reduction in the number of retinal proliferative cells and progenitor cells, as well as a decrease in marker expression, thereby impairing the early development of the retina. At the cellular proliferation level, relevant studies have shown that ischemia inhibits the proliferation of rat brain cells, reduces the expression of Ki67 in brain tissue, and promotes apoptosis in rat brain cells^[30]. Research on zebrafish injury also indicates that ischemia can cause proliferation damage to vascular endothelial cells in zebrafish^[31]. At the stem/progenitor cell level, studies based on mouse models of cerebral ischemia

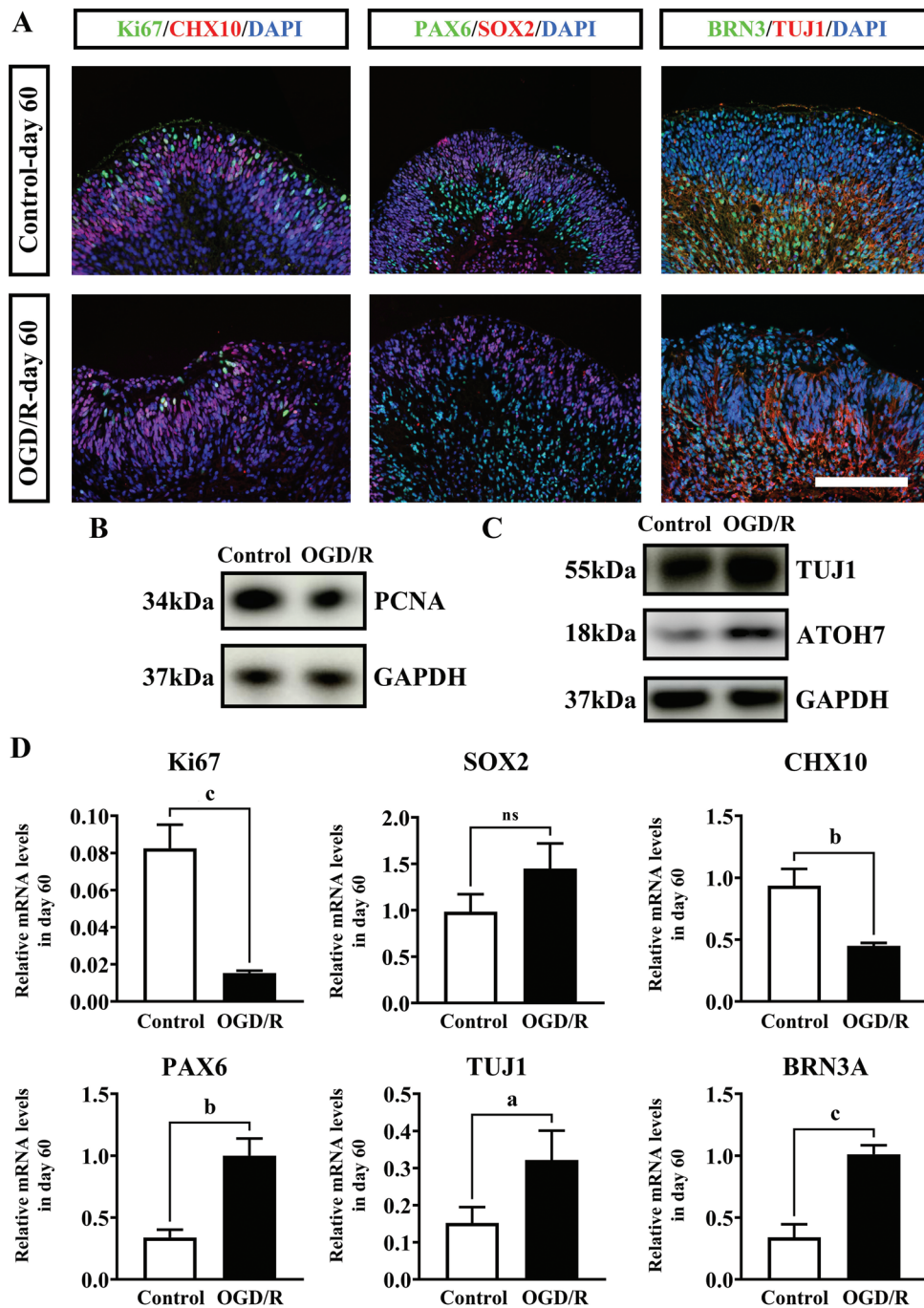


Figure 7 Damage on the development of retina after oxygen-glucose deprivation and reperfusion (OGD/R) treatment on day 18 had a restricted recovery on day 60. A: Representative immunofluorescent images stained for Ki67, CHX10, PAX6, SOX2, TUJ1, BRN3 in neural retina at 200× magnification on day 60. Nuclei were counterstained with DAPI. Ki67: Retinal proliferating cells; SOX2: Retinal neural stem cells; CHX10 and PAX6: Retinal progenitor cells; TUJ1 and BRN3: Retinal ganglion cells. Scale bar: 100 μm. B, C: Representative images of WB stained for proliferative protein PCNA, retinal ganglion cell marker protein ATOH7 and TUJ1 on day 60, normalised by GAPDH. D: Statistical graph of relative mRNA levels of Ki67, CHX10, PAX6, SOX2, TUJ1 and BRN3A, normalised by GAPDH ($n=15$ from three experiments). Error bars represent standard deviations. ^a $P<0.05$; ^b $P<0.01$; ^c $P<0.001$; ns: No significance; WB: Western blot; Ki67: Proliferating cellular marker; PAX6: Paired box gene 6; SOX2: Sex determining region Y box protein 2; CHX10: Retinal progenitor cellular marker; TUJ1: β tubulin III; BRN3: Brain specific homeobox/POU domain protein 3; ATOH7: Human protein atonal homolog 7; DAPI: 4',6-diamidino-2-phenylindole; PCNA: Proliferating cell nuclear antigen; GAPDH: Glyceraldehyde-3-phosphate dehydrogenase.

have revealed that SOX2-positive neural stem cells are crucial protective components of the brain during stroke, and the proportion of neural stem cells in ischemic mouse brains

decreases^[32]. In animal experiments related to early retinal development, retinal progenitor cells have also been identified as sensitive targets of damage^[33]. In studies related to retinal

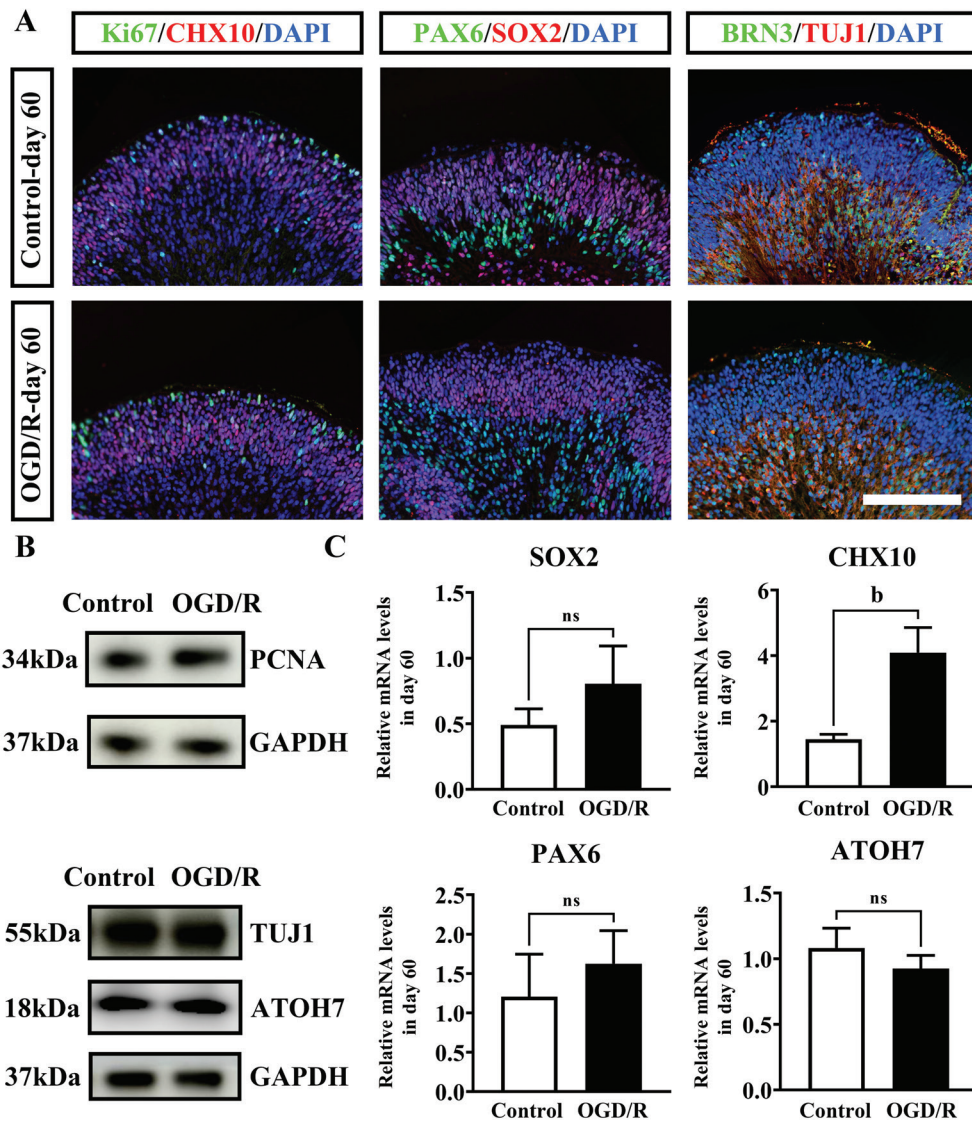


Figure 8 Damages of retina caused by OGD/R treatment on day 30 completely recovered on day 60 A: Representative immunofluorescent images stained for Ki67, CHX10, PAX6, SOX2, TUJ1 and BRN3 in neural retina of two groups at 200× magnification on day 60. Nuclei were counterstained with DAPI. Ki67: Retinal proliferating cells; SOX2: Retinal neural stem cells; CHX10 and PAX6: Retinal progenitor cells; TUJ1 and BRN3: Retinal ganglion cells. Scale bar: 100 μm. B: Representative images of WB stained for proliferative PCNA and retinal ganglion cell marker protein TUJ1 and ATOH7 on day 60, normalised by GAPDH. C: The relative mRNA levels of SOX2, CHX10, PAX6 and ATOH7 on day 60, normalised by GAPDH (n=15 from three experiments). Error bars represent standard deviations. ^bP<0.01; ns: No significance; WB: Western blot; Ki67: Proliferating cellular marker; PAX6: Paired box gene 6; SOX2: Sex determining region Y box protein 2; CHX10: Retinal progenitor cellular marker; TUJ1: β tubulin III; BRN3: Brain specific homeobox/POU domain protein 3; ATOH7: Human protein atonal homolog 7; DAPI: 4',6-diamidino-2-phenylindole; PCNA: Proliferating cell nuclear antigen; GAPDH: Glyceraldehyde-3-phosphate dehydrogenase.

ischemia in humans, as early as 2013, Hellström *et al*^[34] reviewed the ischemic changes in the eyes of children with retinopathy of prematurity caused by hypoxia, and identified that neural retina damage after ischemia is a leading reason for vision loss. Studies on adult ischemic diseases also clarified the damaging effects of ischemia on retinal cells, including the decrease of proliferative cells and SOX2-positive neural stem cells, the increase of apoptosis after TUNEL staining and the loss of neurons^[35-36]. However, these previous studies are mostly based on animal models and mature retina, so their

conclusions may not be conducive for analyzing changes in neonatal retina post ischemia^[37]. In our study, the short-term OGD/R exposure had a key effect on the initial neurogenesis of the neural retina by inhibiting cell proliferation, changing the proportion of stem and progenitor cells and damaging neurons, which is consistent with the inhibition of proliferative cells and the damage of stem progenitor cells reported in previous literature. Meanwhile, our research also indicates that damaged PAX6-positive retinal progenitor cells may undergo abnormal differentiation, a phenotype that is entirely distinct

from that observed in other retinal progenitor cells, which is consistent with previous studies based on brain organoids^[27]. According to previous studies, the developing retina experiences a physiological period of hypoxia during nervous system development^[38]. This hypoxic environment is positively significant for inducing the expression of the retinal precursor gene PAX6 and facilitating retinal cell differentiation^[39-40]. In some studies, hypoxia has also been described as an important reason for inhibiting the proliferation of retinal stem cells and promoting the differentiation and development of retinal stem cells^[41-42]. Therefore, we hypothesize that the elevated expression of PAX6 may be related to the role of hypoxia in initiating neural development and may serve a protective function against damage in ischemic conditions.

Furthermore, the research findings indicate that ischemia leads to the inhibition of retinal ganglion cell migration, a reduction in cell population, and a decrease in the expression of cellular markers, impairing the normal development of ganglion cells. In the study of retinal ischemia in mice, the thinning of the neural retina is primarily characterized by a reduction in the thickness of the ganglion cell layer. Additionally, there is an observed increase in ganglion cell apoptosis and axonal degeneration^[43]. Another study on retinal ischemia in mice also demonstrated an increase in ischemia-induced apoptosis of ganglion cells and discussed the association between ischemic apoptosis of ganglion cells and ferroptosis^[44]. In studies of mature ganglion cells in adults, ganglion cells have been confirmed to be sensitive cells to ischemic retinal injury and are considered as a representative alteration in retinal ischemic damage^[45-46]. In studies related to diabetic retinopathy, researchers have discussed the detrimental changes caused by retinal ischemia in diabetic retinopathy, including vacuolar degeneration and pyroptosis of ganglion cells, as well as the thinning of the ganglion cell layer^[47]. In the research on glaucoma, scholars have also discussed that elevated intraocular pressure can lead to retinal ischemia, increased degeneration and apoptosis of ganglion cells, ultimately resulting in diminished visual function^[48]. However, it is mainly based on the conclusion of mature retina, and the effect on developing immature ganglion cells has not been determined^[49-51]. In our study, we expounded the damaging effects of ischemia on immature retinal ganglion cells, including the axonal defect and the inhibition on retinal ganglion cell development. Moreover, there were short-term ganglion cell injuries in different developmental node ischemic events, which confirmed that ganglion cells are the common feature of short-term ischemic injury of fetal retina.

Simultaneously, this study observed that the damage to retinal cells caused by OGD/R undergoes a certain degree of self-repair during subsequent retinal development, including the

restoration of retinal tissue structure and cellular components. Moreover, the structural and cellular damage in organoids treated with OGD/R at a later stage could be completely restored. These findings suggest that early retinal development may possess a reparative function against ischemic injury, and the extent of self-repair is related to the timing of the ischemic event, with earlier ischemic injuries being more difficult to repair^[52]. Literature indicates that the reparative effects during retinal development may be associated with glial cells. Studies based on zebrafish have shown that glial cells in the retina may have the capacity to repair retinal damage, as they can maintain the internal homeostasis of the retina, creating conditions for retinal regeneration. Additionally, these cells can secrete relevant signaling molecules that promote retinal cell proliferation and repair, maintaining retinal integrity^[53]. Research on zebrafish retina has also discussed the reparative role of glial cells in retinal damage, manifested through the promotion of ganglion cell differentiation and axon extension *via* the PI3K-AKT pathway^[23]. In the treatment of glaucoma and diabetic retinopathy, it has been shown that activating glial cells can repair damage to ganglion cells^[54-55]. In our study, the self-repair capability of early retinal development was validated using hROs. However, although glial cells can be induced to proliferate and generate neurons under specific conditions, studies have shown that this damage repair response is relatively weak and insufficient to repair the damaged retina in mammals^[56]. Therefore, the mechanisms underlying damage repair during the development of hROs require further investigation.

In summary, this study has revealed the damaging effects of ischemia on the early retina. This finding suggests that clinical practitioners need to promptly pay attention to and assess the ocular damage in infants suffering from intrauterine distress. Furthermore, in clinical practice, restoring blood supply is a primary rescue measure to save the lives of infants with intrauterine distress^[9], and this research also indicate that after the retina regains normal blood supply, retinal ischemic damage can be repaired to varying degrees during long-term development, suggesting that restoring blood supply is equally important for the ocular prognosis of these infants. However, high-concentration oxygen therapy is also a direct cause of clinical retinopathy of prematurity and aggravated retinal damage, necessitating more research to provide reasonable oxygen therapy strategies^[57]. Additionally, we have documented the recovery of organoids with different ischemia onset times during long-term development and found that earlier ischemia may lead to a better prognosis. This result coincides with the conclusion from clinical studies that the prognosis of intrauterine distress may be related to gestational age, indicating that clinical practitioners need to strengthen

the monitoring of infants with intrauterine distress at lower gestational ages to reduce sequelae.

ACKNOWLEDGEMENTS

Foundation: Supported by the National Natural Science Foundation of China (No.82070937).

Conflicts of Interest: Yan YH, None; Li HY, None; Gao LX, None; Li W, None; Zhao LP, None; Zeng Q, None; Luo Y, None; Cui TT, None; Zang RG, None; Ye Z, None; Xi JF, None; Yue W, None; Li ZH, None.

REFERENCES

- 1 Tong YJ, Zhang SQ, Riddle S, *et al.* Intrauterine hypoxia and epigenetic programming in lung development and disease. *Biomedicines* 2021;9(8):944.
- 2 Raicević S, Cubrilo D, Arsenijević S, *et al.* Oxidative stress in fetal distress: potential prospects for diagnosis. *Oxid Med Cell Longev* 2010;3(3):214-218.
- 3 Schaap AH, Wolf H, Bruinse HW, *et al.* Fetal distress due to placental insufficiency at 26 through 31 weeks: a comparison between an active and a more conservative management. *Eur J Obstet Gynecol Reprod Biol* 1996;70(1):61-68.
- 4 Pu QL, Zhou QY, Liu J, *et al.* Clinical observation and related factors analysis of neonatal asphyxia complicated with retinal hemorrhage. *Zhonghua Yan Ke Za Zhi* 2017;53(5):358-362.
- 5 Dorweiler TF, Singh A, Ganju A, *et al.* Diabetic retinopathy is a ceramidopathy reversible by anti-ceramide immunotherapy. *Cell Metab* 2024;36(7):1521-1533.e5.
- 6 Xie Z, Ying Q, Luo HD, *et al.* Resveratrol alleviates retinal ischemia-reperfusion injury by inhibiting the NLRP3/gasdermin D/caspase-1/interleukin-1 β pyroptosis pathway. *Invest Ophthalmol Vis Sci* 2023;64(15):28.
- 7 Chen C, Singh G, Madike R, *et al.* Central retinal artery occlusion: a stroke of the eye. *Eye (Lond)* 2024;38(12):2319-2326.
- 8 Minhas G, Sharma J, Khan N. Cellular stress response and immune signaling in retinal ischemia-reperfusion injury. *Front Immunol* 2016;7:444.
- 9 Chen J, Liu FX, Tao RX. Relationship between ultrasound parameters of the umbilical and middle cerebral arteries and intrauterine fetal distress. *World J Clin Cases* 2024;12(16):2745-2750.
- 10 Lakhno IV, Uzel K. Diagnosing antenatal fetal distress. *Ginekol Pol* 2022;93(1):54-56.
- 11 Wu XD, Yu NJ, Ye ZF, *et al.* Inhibition of cGAS-STING pathway alleviates neuroinflammation-induced retinal ganglion cell death after ischemia/reperfusion injury. *Cell Death Dis* 2023;14(9):615.
- 12 Pang YL, Hu HJ, Xu K, *et al.* CD38 deficiency protects mouse retinal ganglion cells through activating the NAD⁺/Sirt1 pathway in ischemia-reperfusion and optic nerve crush models. *Invest Ophthalmol Vis Sci* 2024;65(5):36.
- 13 Shahror RA, Shosha E, Morris C, *et al.* Deletion of myeloid HDAC3 promotes efferocytosis to ameliorate retinal ischemic injury. *J Neuroinflammation* 2024;21(1):170.
- 14 Norrie JL, Nityanandam A, Lai KR, *et al.* Retinoblastoma from human stem cell-derived retinal organoids. *Nat Commun* 2021;12(1):4535.
- 15 Spirig SE, Renner M. Toward retinal organoids in high-throughput. *Cold Spring Harb Perspect Med* 2024;14(3):a041275.
- 16 Duan CW, Ding CC, Sun XH, *et al.* Retinal organoids with X-linked retinoschisis RS1 (E72K) mutation exhibit a photoreceptor developmental delay and are rescued by gene augmentation therapy. *Stem Cell Res Ther* 2024;15(1):152.
- 17 Zhao N, Zhang CJ, Zhang X, *et al.* Transplantation of derivative retinal organoids from chemically induced pluripotent stem cells restored visual function. *NPJ Regen Med* 2024;9(1):42.
- 18 O'Hara-Wright M, Gonzalez-Cordero A. Retinal organoids: a window into human retinal development. *Development* 2020;147(24):dev189746.
- 19 Romano C, Price M, Bai HY, *et al.* Neuroprotectants in Honghua: glucose attenuates retinal ischemic damage. *Invest Ophthalmol Vis Sci* 1993;34(1):72-80.
- 20 Ye XY, Liu YF, Chen CY, *et al.* A novel function and mechanism of ischemia-induced retinal astrocyte-derived exosomes for RGC apoptosis of ischemic retinopathy. *Mol Ther Nucleic Acids* 2024;35(2):102209.
- 21 Zeng Z, You ML, Fan C, *et al.* Pathologically high intraocular pressure induces mitochondrial dysfunction through Drp1 and leads to retinal ganglion cell PANoptosis in glaucoma. *Redox Biol* 2023;62:102687.
- 22 Emmerich K, Hageter J, Hoang T, *et al.* A large-scale CRISPR screen reveals context-specific genetic regulation of retinal ganglion cell regeneration. *Development* 2024;151(15):dev202754.
- 23 Subramani M, Lambrecht B, Ahmad I. Human microglia-derived proinflammatory cytokines facilitate human retinal ganglion cell development and regeneration. *Stem Cell Reports* 2024;19(8):1092-1106.
- 24 Zhang J, Qin YW, Martinez M, *et al.* HIF-1 α and HIF-2 α redundantly promote retinal neovascularization in patients with ischemic retinal disease. *J Clin Invest* 2021;131(12):e139202.
- 25 Li HY, Gao LX, Ye Z, *et al.* Protective effects of resveratrol on the ethanol-induced disruption of retinogenesis in pluripotent stem cell-derived organoids. *FEBS Open Bio* 2023;13(5):845-866.
- 26 Li W, Li HY, Yan H, *et al.* Generating neural retina from human pluripotent stem cells. *J Vis Exp* 2023(202).
- 27 Wang SN, Wang Z, Wang XY, *et al.* Humanized cerebral organoids-based ischemic stroke model for discovering of potential anti-stroke agents. *Acta Pharmacol Sin* 2023;44(3):513-523.
- 28 Iwasa N, Matsui TK, Iguchi N, *et al.* Gene expression profiles of human cerebral organoids identify PPAR pathway and PKM2 as key markers for oxygen-glucose deprivation and reoxygenation. *Front Cell Neurosci* 2021;15:605030.
- 29 Shi SJ, Roest HP, van den Bosch TPP, *et al.* Modeling bile duct ischemia and reoxygenation injury in human cholangiocyte organoids for screening of novel cholangio-protective agents. *EBioMedicine* 2023;88:104431.

- 30 Cui YX, Cui MY, Wang LL, *et al.* Huanglian Jiedu decoction alleviates ischemia-induced cerebral injury in rats by mitigating NET formation and activating GABAergic synapses. *J Cell Mol Med* 2024;28(15):e18528.
- 31 Wang YQ, Wang SH, Wang YH, *et al.* The natural compound sinometumine E derived from *Corydalis decumbens* promotes angiogenesis by regulating HIF-1/VEGF pathway *in vivo* and *in vitro*. *Biomedicine Pharmacother* 2024;178:117113.
- 32 Xu J, Wang TT, Guo FF, *et al.* Systematical identification of the protective effect of Danhong injection and BuChang NaoXinTong capsules on transcription factors in cerebral ischemia mice brain. *Oxid Med Cell Longev* 2020;2020:5879852.
- 33 Taguchi K, Watanabe Y, Tsujimura A, *et al.* α -synuclein promotes maturation of immature juxtglomerular neurons in the mouse olfactory bulb. *Mol Neurobiol* 2020;57(3):1291-1304.
- 34 Hellström A, Smith LE, Dammann O. Retinopathy of prematurity. *Lancet* 2013;382(9902):1445-1457.
- 35 Jassim AH, Fan Y, Pappenhagen N, *et al.* Oxidative stress and hypoxia modify mitochondrial homeostasis during glaucoma. *Antioxid Redox Signal* 2021;35(16):1341-1357.
- 36 Xin X, Dang H, Zhao X, *et al.* Effects of hypobaric hypoxia on rat retina and protective response of resveratrol to the stress. *Int J Med Sci* 2017;14(10):943-950.
- 37 Caprara C, Grimm C. From oxygen to erythropoietin: relevance of hypoxia for retinal development, health and disease. *Prog Retin Eye Res* 2012;31(1):89-119.
- 38 Chan-Ling T, Gock B, Stone J. The effect of oxygen on vasoformative cell division. Evidence that 'physiological hypoxia' is the stimulus for normal retinal vasculogenesis. *Invest Ophthalmol Vis Sci* 1995;36(7):1201-1214.
- 39 Buttery RG, Hinrichsen CFL, Weller WL, *et al.* How thick should a retina be A comparative study of mammalian species with and without intraretinal vasculature. *Vis Res* 1991;31(2):169-187.
- 40 Flammer J, Mozaffarieh M. Autoregulation, a balancing act between supply and demand. *Can J Ophthalmol* 2008;43(3):317-321.
- 41 Yasan GT, Gunel-Ozcan A. Hypoxia and hypoxia mimetic agents as potential priming approaches to empower mesenchymal stem cells. *Curr Stem Cell Res Ther* 2024;19(1):33-54.
- 42 Du JL, Gao LX, Wang T, *et al.* Influence of hypoxia on retinal progenitor and ganglion cells in human induced pluripotent stem cell-derived retinal organoids. *Int J Ophthalmol* 2023;16(10):1574-1581.
- 43 Jiang N, Li ZD, Li ZH, *et al.* Laquinimod exerts anti-inflammatory and antiapoptotic effects in retinal ischemia/reperfusion injury. *Int Immunopharmacol* 2020;88:106989.
- 44 Qin QY, Yu NJ, Gu YX, *et al.* Inhibiting multiple forms of cell death optimizes ganglion cells survival after retinal ischemia reperfusion injury. *Cell Death Dis* 2022;13(5):507.
- 45 Osborne NN, Ugarte M, Chao M, *et al.* Neuroprotection in relation to retinal ischemia and relevance to glaucoma. *Surv Ophthalmol* 1999;43(Suppl 1):S102-S128.
- 46 Sellés-Navarro I, Villegas-Pérez MP, Salvador-Silva M, *et al.* Retinal ganglion cell death after different transient periods of pressure-induced ischemia and survival intervals. A quantitative *in vivo* study. *Invest Ophthalmol Vis Sci* 1996;37(10):2002-2014.
- 47 Li N, Guo XL, Xu M, *et al.* Network pharmacology mechanism of Scutellarin to inhibit RGC pyroptosis in diabetic retinopathy. *Sci Rep* 2023;13(1):6504.
- 48 Bou Ghanem GO, Wareham LK, Calkins DJ. Addressing neurodegeneration in glaucoma: Mechanisms, challenges, and treatments. *Prog Retin Eye Res* 2024;100:101261.
- 49 Cen LP, Park KK, So KF. Optic nerve diseases and regeneration: how far are we from the promised land. *Clin Exp Ophthalmol* 2023;51(6):627-641.
- 50 Chen H, Deng Y, Gan XL, *et al.* NLRP12 collaborates with NLRP3 and NLRC4 to promote pyroptosis inducing ganglion cell death of acute glaucoma. *Mol Neurodegener* 2020;15(1):26.
- 51 Zhao R, He T, Xing Y, *et al.* COG1410 regulates microglial states and protects retinal ganglion cells in retinal ischemia-reperfusion injury. *Exp Eye Res* 2023;237:109678.
- 52 Hoang T, Wang J, Boyd P, *et al.* Gene regulatory networks controlling vertebrate retinal regeneration. *Science* 2020;370(6519):eabb8598.
- 53 Barrett LM, Mitchell DM, Meighan PC, *et al.* Dynamic functional and structural remodeling during retinal regeneration in zebrafish. *Front Mol Neurosci* 2022;15:1070509.
- 54 Margeta MA, Yin ZR, Madore C, *et al.* Apolipoprotein E4 impairs the response of neurodegenerative retinal microglia and prevents neuronal loss in glaucoma. *Immunity* 2022;55(9):1627-1644.e7.
- 55 Rolev KD, Shu XS, Ying Y. Targeted pharmacotherapy against neurodegeneration and neuroinflammation in early diabetic retinopathy. *Neuropharmacology* 2021;187:108498.
- 56 Goldman D. Müller glial cell reprogramming and retina regeneration. *Nat Rev Neurosci* 2014;15(7):431-442.
- 57 Hofmeyr GJ. Maternal oxygen administration for fetal distress. *Cochrane Database Syst Rev* 2000(2):CD000136.